FRONTIERS OF PHYSICS

RESEARCH ARTICLE
Volume 17 / Issue 6 / 62503 / 2022

A calibration-free model for laser-induced breakdown spectroscopy using non-gated detectors

Zongyu Hou[1,2], Weilun Gu[1,2], Tianqi Li[1,2], Zhe Wang[1,2,†], Liang Li[3], Xiang Yu[4], Yecai Zhang[5], Zijun Liu[6]

1 State Key Lab of Power System, Department of Energy and Power Engineering, International Joint Laboratory on Low Carbon Clean Energy Innovation, Tsinghua University, Beijing 100084, China
2 Shanxi Research Institute for Clean Energy, Tsinghua University, Taiyuan 030032, China
3 Beijing Research Institute of Chemical Engineering and Metallurgy, Beijing 101149, China
4 China National Uranium Corporation, Beijing 100013, China
5 Guoneng Shenwan Energy Co., Ltd, China
6 Jinneng Holding Tashan Power Generation Co., Ltd, China
Corresponding author. E-mail: †zhewang@tsinghua.edu.cn
Received July 5, 2022; accepted July 27, 2022

ABSTRACT

Calibration-free (CF) laser-induced breakdown spectroscopy (LIBS) is normally only applicable for gated detectors due to its dependence on the assumption of a steady-state plasma. However, most currently available LIBS systems are equipped with non-gated detectors such as charge-coupled device (CCD), which degrades the accuracy of CF method. In this paper, the reason for the less satisfactory quantification performance of CF for LIBS with non-gated detectors was clarified and a time-integration calibration-free (TICF) model was proposed for applications with non-gated detectors. It was based on an assumed temporal profile of plasma properties, including temperature and electron density, obtained from another pre-experiment. The line intensity at different time during the signal collection time window was estimated with self-absorption correction according to the temporal profile of the plasma properties. The proposed model was validated on titanium alloys and compared with traditional CF. The accuracy of elemental concentration measurement was improved significantly: the average relative error of aluminum and vanadium decreased from 6.07% and 22.34% to 2.01% and 1.92%, respectively. The quantification results showed that TICF method was able to extend the applicability of CF to LIBS with non-gated detectors.

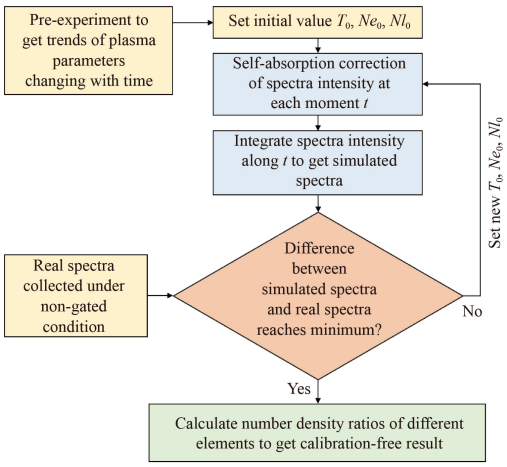

Keywords laser-induced breakdown spectroscopy, calibration-free, non-gated detector, self-absorption correction

1 Introduction

Laser-induced breakdown spectroscopy (LIBS) has been regarded as one of the most versatile elemental analysis techniques and has shown great potential in many applications [1–4], such as metals [5], coal [6], pollutants [7], and minerals [8]. Generally, quantitative LIBS analysis is performed by calibration models [9–14] and calibration-free (CF) models [15–18]. The CF model proposed by Ciucci *et al.* [17] avoids the use of a series of reference samples and thus improves the convenience of LIBS. However, the CF model relies on strict assumptions,

Higher Education Press

https://doi.org/10.1007/s11467-022-1195-9

including stoichiometric ablation, optical thinness (free of self-absorption), and spatial homogeneity and local thermodynamic equilibrium (LTE) of the plasma [19]. There is also an implicit assumption of a steady state plasma because the drastically changing plasma temperature and electron density are not considered in the CF model, since lumped constant temperature and electron density are applied. In general, emission with tens to thousands of nanoseconds of the earlier stage plasma is collected using gated signal detectors such as intensified charge-coupled device (ICCD) to meet the LTE condition and the nearly steady state assumption [19–21]. However, most currently available LIBS systems are equipped with non-gated detectors such as charge-coupled device (CCD) for their low cost and high stability, with an exposure time about 1 millisecond and do not satisfy the basic assumptions. Despite the possible violation of CF assumptions, some researchers attempted CF model with CCD detectors [22–26], but the quantification performance were not satisfactory compared with those with ICCD detectors. Grifoni *et al.* [27] proposed to obtain time-resolved spectra by the subtraction between two LIBS spectra at two different delays using a CCD detector. Although this method does not require any pre-calibration of the system and does not rely on theoretical assumptions or iterative procedures, the subtraction between two LIBS spectra actually increases the uncertainty of signal since essentially these two spectra were obtained from two different laser-induced plasmas, which is absolutely harmful to the final results. In addition, the line intensity estimated from subtraction may sometimes be very weak or even be negative, limiting its potential for CF analysis. The application of CF model for LIBS with CCD detectors is still a big challenge for LIBS.

Another problem which affects the quantification performance of CF is self-absorption [20, 28]. Self-absorption is an undesirable phenomenon in which plasma emission is re-absorbed by the plasma itself. It generally reduces the intensity and increases the width of an emission spectral line, resulting in inaccurate estimation of plasma temperature and elemental concentrations in CF-LIBS [29–33]. Various methods have been proposed to correct the self-absorption effect [34]. Bulajic *et al.* [35] used curve of growth (COG) for self-absorption correction, in which the effect of self-absorption on line profile was clarified and an iterative algorithm was proposed to calculate plasma temperature, electron number density, Gaussian broadening, Lorentzian broadening, and optical path length. Based on this method, Sherbini *et al.* [36] summarized the relationship between line broadening and self-absorption extent, and proposed a simplified iterative algorithm to correct self-absorption, but required at least one optically thin line with negligible self-absorption effect. Aragon *et al.* [37] applied a C-sigma method to compensate for the self-absorption effect and quantitatively analyzed elements in aluminum alloys. Moon *et al.* [38] proposed a duplicating mirror method to measure and correct self-absorption, but required an additional mirror and an optical shutter, and required to collect spectra with and without the mirror each time. Sun *et al.* [22] proposed a method that used one or several lines as internal reference, which were regarded free from self-absorption, for self-absorption correction (IRSAC), while the intensity of other lines was calculated by the reference line intensity and the plasma temperature was estimated based on theoretical equation. Dong *et al.* [16] proposed the internal reference –external standard with the iteration correction (IRESIC) procedure based on IRSAC, in which one matrix-matched standard sample along with the genetic algorithm (GA) was utilized to estimate the accurate plasma temperature. Demidov *et al.* [39] proposed an improved Monte-Carlo (MC) method for standard-less analysis, where the concentrations were found by fitting model-generated synthetic spectra to experimental spectra. Zhu *et al.* [40] proposed an approach to overcome the self-absorption effect by utilizing molecular emission. Li *et al.* [41] proposed a new self-absorption correction method for CF-LIBS called blackbody radiation referenced self-absorption correction (BRR-SAC). It used an iterative algorithm to calculate the plasma temperature and the normally hard-to-obtain collection efficiency of the optical collection system by directly comparing the measured spectrum with the corresponding theoretical blackbody radiation for self-absorption correction.

However, none of these correction methods considered the influence of plasma evolution on the degree of self-absorption. Plasma properties such as temperature and electron density changes drastically during the exposure time of non-gated detectors [42–44]. The self-absorption also changes drastically due to the change of temperature and electron density [45], making the normal self-absorption correction methods not applicable for non-gated detectors. In this paper, a new CF model with self-absorption correction that can be used under non-gated conditions is proposed, namely time-integration calibration-free (TICF), and is applied for titanium alloy samples. The results show that TICF can effectively improve the measurement accuracy compared to traditional CF.

2 Methods

According to the theory of plasmas in LTE, the emission intensity ε (W m^{-1}) of the line with the central wavelength of λ_0 (m) can be expressed as [46]

$$\varepsilon(\lambda) = F \cdot \frac{hc}{4\pi\lambda_0} gA \cdot \frac{rNl}{U(T)} \exp\left(-\frac{E}{kT}\right) V(\lambda), \qquad (1)$$

and its wavelength-integrated emission intensity I(W) is

$$I = \int \varepsilon(\lambda)\mathrm{d}\lambda = F \cdot \frac{hc}{4\pi\lambda_0} gA \cdot \frac{rNl}{U(T)} \exp\left(-\frac{E}{kT}\right). \quad (2)$$

where F (m^2) is the coefficient of collection that takes into account the optical efficiency of the collection system as well as the region of the plasma in the viewing field of optical collection system [47], h (J·s) is the Planck constant, c ($m \cdot s^{-1}$) is the speed of light in vacuum, and k ($J \cdot K^{-1}$) is the Boltzmann constant. A (s^{-1}) is the transition probability, g (dimensionless) and E (J) are the degeneration and the energy of the upper level of the transition, respectively, and U (dimensionless) is the partition function of the emitting species. T (K) is the plasma temperature, N (m^{-3}) is the elemental number density, l (m) is the plasma length, r (dimensionless)is the ionization factor of the emitting species, which represents the percentage of emitting species to the corresponding elemental species and can be obtained by the Saha-Boltzmann ionization equation, and $V(\lambda)$ is the normalized spectral line profile. It should be noted that since N and l always appear at the same time, Nl (m^{-2}) will be merged into one variable (columnar density) in the following discussion.

The representation of $\ln[I\lambda_0/gA]$ as a function of E, called a Boltzmann plot, leads to a straight line with a negative slope $-1/(kT)$ and an intercept that characterizes the number of species, from which the temperature and elemental concentration can be obtained.

For non-gated LIBS, we treat the plasma as an evolving object with universal temporal profile for fixed experimental setup but spatially homogeneous. The expressions for plasma temperature, electron density, and number of species at moment t are

$$T(t) = f_T(T_0, t), \quad (3)$$

$$N_e(t) = f_{Ne}(N_{e0}, t), \quad (4)$$

$$Nl(t) = f_{Nl}(Nl_0, t). \quad (5)$$

where f_T, f_{Ne} and f_{Nl} represent the profile function of the change of plasma temperature, electron density, and particle number density with time, respectively. T_0, N_{e0} and Nl_0 represent the parameters of the plasma at a certain delay time (the moment when we start to characterize the plasma evolution), which depends on and needs to be determined for each different sample. In this paper, a time-resolved pre-experiment with ICCD is used to determine the expression of f_T, f_{Ne} and f_{Nl}. Considering the temporal evolution, the expression of the intensity I in Equation 2 should be corrected to

$$I = F \cdot \frac{hc}{4\pi\lambda_0} gA \cdot \int \frac{r(t)Nl(t)}{U(T(t))} \exp\left(-\frac{E}{kT(t)}\right) V(\lambda, t)\,\mathrm{d}t, \quad (6)$$

The potential self-absorption effect of the plasma leads to the failure of the optical thinness assumption, which usually weakens the intensity of the spectral line and should be corrected. For spectrum collected under non-gated conditions, the plasma temperature T and electron number density N_e change along plasma evolution process, which leads to changes of self-absorption effect [48, 49]. A simple simulation of the self-absorption (SA) coefficient defined by Ref. [32] of Al(I) 394.4 nm changing with T and N_e is shown in Fig. 1, which helps to understand the change of self-absorption effect under non-gated conditions. Significant changes in self-absorption coefficient can be observed in the typical ranges of T and N_e during the exposure time of non-gated detectors, which indicates the urgent need of self-absorption correction and the inapplicability of existing correction methods. Therefore, it is necessary to introduce and to improve the self-absorption correction for the CF-LIBS under non-gated conditions.

Self-absorption correction can be achieved by comparing the intensity of the plasma emission with the intensity of the blackbody radiation at the corresponding temperature. Our previous work [41] has elaborated on the principles of self-absorption correction and proposed a method called blackbody radiation referenced self-absorption correction (BRR-SAC) method. The basic idea of BRR-SAC is to imagine an ideal blackbody which has the same temperature as the plasma. By comparing the emission of the ideal blackbody and the plasma, the self-absorption effect can be evaluated and corrected. The plasma emission intensity with and without

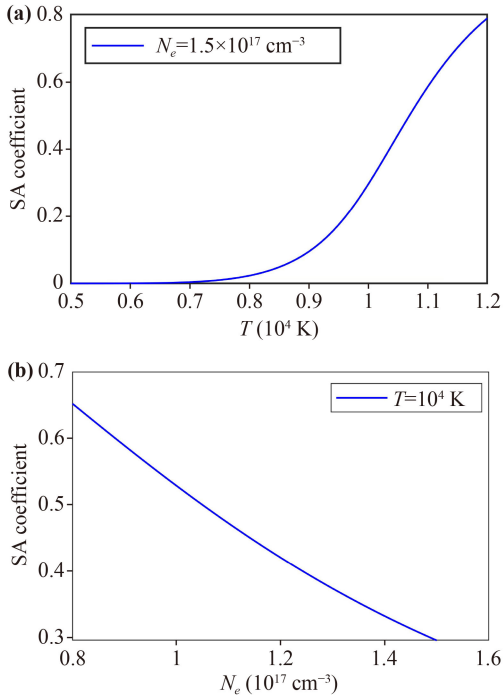

Fig. 1 Self-absorption (SA) coefficient simulation of Al(I) 394.4 nm changing with T **(a)** and N_e **(b)** (pure Al sample, plasma size 2 mm).

self-absorption effect can be described as a function of blackbody radiation intensity $L_P(\lambda)$ and optical length $\tau(\lambda)$:

$$L_P(\lambda) = \frac{2\pi hc^2}{\lambda^5}\frac{1}{e^{hc/(\lambda kT)}-1}, \quad (7)$$

$$\varepsilon(\lambda) = F \cdot L_P(\lambda)\,\tau(\lambda), \quad (8)$$

$$\varepsilon^*(\lambda) = F \cdot L_P(\lambda)\left[1 - e^{-\tau(\lambda)}\right], \quad (9)$$

where $\varepsilon(\lambda)$ is the emission intensity without self-absorption and has the same meaning as in Eq. (1) while $\varepsilon^*(\lambda)$ is the emission intensity which considers the self-absorption effect. The intensity I^* after considering the self-absorption effect can be obtained by integrating $\varepsilon^*(\lambda)$ along time and wavelength:

$$I^* = F\iint L_P(\lambda,t)\left\{1-\exp\left[-\frac{1}{L_P(\lambda,t)}\frac{hc}{4\pi\lambda_0}gA \times \frac{r(t)Nl(t)}{U(T(t))}\exp\left(-\frac{E}{kT(t)}\right)V(\lambda,t)\right]\right\}d\lambda dt, \quad (10)$$

In addition, the broadening of spectral line profile should be considered since it was affected by self-absorption. In this study, Stark broadening is considered as the main factor for the broadening of line profile, and the expression for $V(\lambda, t)$ is

$$V(\lambda,t) = \frac{1}{\pi\gamma(t)}\left[\frac{\gamma^2(t)}{(\lambda-\lambda_0)^2+\gamma^2(t)}\right]. \quad (11)$$

where γ is the scale parameter which specifies the half-width at half-maximum (HWHM) and can be expressed as a function of electron density N_e and Stark broadening coefficient α:

$$\gamma(t) = \frac{1}{2}\alpha N_e(t). \quad (12)$$

Since the Stark broadening coefficient α is not available or not accurate in many cases, it is set as an unknown variable in this study. Considering the strong positive correlation between α and the HWHM of a certain spectral line and the little effect of α on the wavelength-integrated intensity, α can be quickly adjusted to make the HWHM of the calculated line the same as the experimental line.

Based on the above derivation, the new CF procedure considering temporal evolution, namely TICF, is proposed and described as follows. Iterate the value of T_0, N_{e0}, and Nl_0, until the experimental spectral intensity is as close as possible to that described in Equation 10. Then, these parameters (T_0, Nl_0, and N_{e0}) can be substituted into Equation 6 to obtain the spectral intensity after self-absorption correction. The quantification results can be obtained by the relative number densities of different element by Nl_0. The main procedure of TICF is shown in Fig. 2.

3 Experimental

A standard LIBS setup was used in this experiment. A Q-switched Nd:YAG laser (Q-Smart 100, Quantel, France) was applied. The laser wavelength was 1064 nm and energy was set to 80 mJ/pulse, with a pulse duration of 6 ns and a repetition rate of 1 Hz. The spot size at the sample surface was about 0.2 mm in diameter. A spectrometer with non-gated CCD detectors (Avantes, Netherland) was used to acquire plasma spectra. The wavelength range of spectra was from 180 to 430 nm and the spectral resolution about 0.1 nm. Optical fiber and spectrometer were corrected by a standard light

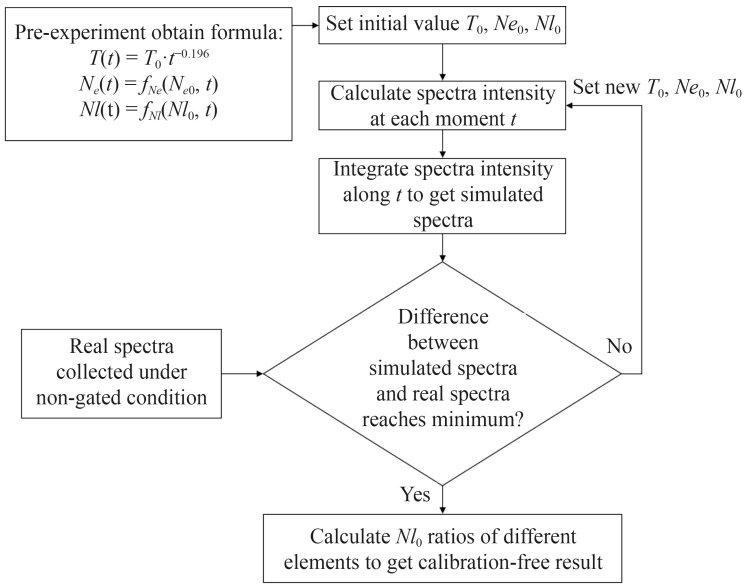

Fig. 2 Main procedure of TICF.

source (DH-3plus, Ocean Tec, USA). The sample was standard titanium alloys (Chinese National Standard No.02503~02507) with known concentrations, as shown in Table 1.

To determine the form of the function f_T, f_{Ne} and f_{Nl}, a time-resolved pre-experiment with ICCD (LTB butterfly echelle spectrometer) was performed. Spectra of sample 1# were collected at delay times of 2, 3,...,14, 15, 17 and 20 μs with gate time of 0.1 μs. A short gate time was chosen to avoid strong changes in plasma temperature and electron number density during the measurement. Ten spectra were collected at each delay time and each spectrum is accumulated by 10 laser pulse signals to improve the signal-to-noise ratio.

For all samples, 10 non-gated spectra were collected at the delay time of 2 μs with the exposure time of 1 ms. Each spectrum was generated by a single pulse.

4 Result and discussion

Analytical lines selection. Due to the presence of titanium and vanadium element in the plasma is mainly in the form of ions, a number of titanium ion lines and vanadium ion lines can be found in the spectrum with high intensity. At the same time, several low-intensity titanium and aluminum atomic lines can also be observed. The selected lines for these four species are listed in Table 2. The transition probability A_{ki} is an important parameter of the spectral line, which can be obtained by the NIST database.

Determination of f_T, f_{Ne} and f_{Nl}. For the spectrum of sample 1 with short gate, the temperature can be determined by Boltzmann plots. In order to eliminate the interference of self-absorption effects on these parameters, blackbody radiation referenced self-absorption correction method [41] was applied.

The electron density is obtained by the Saha–Bolzmann ionization equation:

$$n_e = \frac{2(2\pi m_e kT)^{3/2}}{h^3} \frac{I^I_{mn} A_{ij} g_i^{II}}{I^I_{ij} A_{mn} g_m^I} \exp\left(-\frac{E_{ion} + E_i^{II} - E_m^I}{kT}\right). \tag{13}$$

Here, m_e, k, T, and h are the mass of an electron, the Boltzmann constant, the temperature of the plasma, and the Planck's constant, respectively. I_{mn}, A_{mn}, $g_m{}^I$ and $E_m{}^I$ are the observed intensity of the line transition from m-level to n-level, the Einstein coefficient of transition of transition probability for spontaneous transition, the degeneracy of the upper level, and the energy of the upper energy level of an atomic line. Similarly, I_{ij}, A_{ij}, $g_i{}^{II}$ and $E_i{}^{II}$ are parameters of an ionic line. E_{ion} is the 1st ionization energy. Electron density was obtained by substituting data of titanium atom lines and titanium ion lines.

Figure 3 shows the profile of temperature T and the electron density N_e of sample 1# changing with delay time. According to the curve trend of T and N_e in Figure 3, we select power function to fit the curve. The results are as follows:

$$T(t) = T_0 \cdot t^{-0.196}, \tag{14}$$

Table 1 Elemental concentration (wt%) of the samples.

Serial Number	Al	V	Fe	Si	C
1# (GBW02503)	3.90	5.65	0.390	0.277	0.158
2# (GBW02504)	4.67	5.01	0.314	0.196	0.119
3# (GBW02505)	5.38	3.41	0.239	0.115	0.095
4# (GBW02506)	6.48	4.46	0.143	0.052	0.051
5# (GBW02507)	6.78	3.85	0.131	0.085	0.023

Table 2 The selected line of Ti II, V II, Ti I and Al I.

Species	Wavelength(nm)							
Ti II	252.560	252.975	253.125	253.462	253.587	257.103	283.218	284.193
	285.110	288.410	301.718	302.973	304.668	307.522	309.718	310.380
	310.508	310.623	311.980	315.225	316.852	319.087	320.253	321.705
	321.827	322.284	322.424	323.228	324.198	324.860	325.425	328.233
	330.880	331.532	331.802	332.170	332.293	332.676	332.945	333.211
	333.519	334.674	339.457	340.242	340.981	345.246	345.638	347.718
	349.105	350.489	351.084	352.025	353.541	357.373	358.713	359.605
	365.976	366.223	374.164	390.054	391.346			
V II	268.795	270.093	290.308	290.882	295.207	296.838	309.310	310.230
	311.071	313.333	313.494	313.652	351.730	354.520		
Ti I	395.633	395.820	398.176	398.976				
Al I	394.400	396.152						

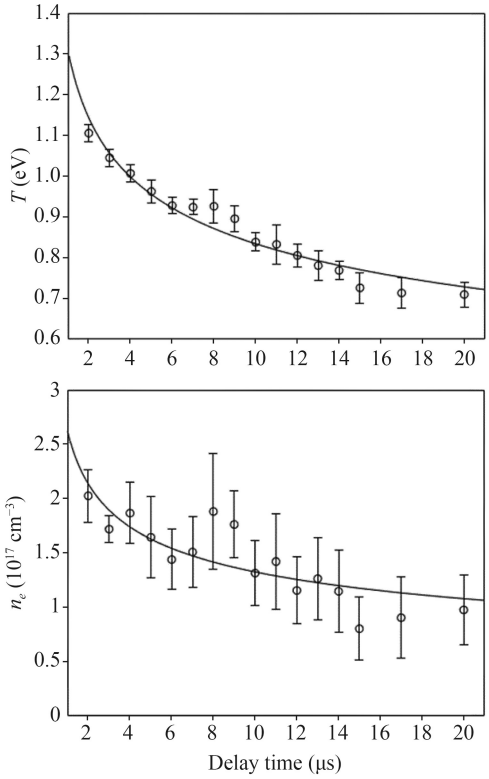

Fig. 3 The profile of temperature T and the electron density N_e change with the delay time.

$$N_e(t) = N_{e0} \cdot t^{-0.296}. \quad (15)$$

The curve of T and N_e for other samples was selected as the same form as formula 14 and 15 since the samples in Table 1 have similar matrices, while T_0 and N_{e0} are to be determined for each sample. The LTE condition of plasma was verified before quantitative analysis. The necessary condition of LTE can be expressed by McWhirter's criterion [50]:

$$n_e > 1.4 \times 10^{14} T^{1/2} (\Delta E)^3 \text{cm}^{-3}, \quad (16)$$

where ΔE (eV) is the highest energy difference between the upper and lower energy levels. According to the formula 16, the critical value of the electron density is 4×10^{16} cm^{-3}, which shows that the plasma in this experiment meets the necessary condition of the local thermal equilibrium. It should be noted that McWhirter criterion is just a necessary condition for LTE, while two additional conditions (relaxation time and diffusion length) are needed to guarantee the LTE conditions [50]. Maybe the additional sufficient conditions of LTE (relaxation time and diffusion length) were difficult to be maintained at 20 microseconds. However, considering the fact that spectral line intensity decreased sharply with time and the main contribution of line intensity was the plasma at early delay which was easier to be at LTE condition [51], it should not be a big problem for CF, and the high accuracy of final CF result showed that this problem can be neglected in this work.

Nl actually represents the number of observed species, and is considered to be independent of time approximately:

$$Nl\,(t) = Nl_0. \quad (17)$$

Quantitative analysis. Here, the calibration-free method is used for quantitative analysis, that is, the elemental concentration is determined according to the elemental number density Nl_0. Since there are multiple lines, we need to adjust the value of T_0, Nl_0, and N_{e0} to minimize the residual error Δ of the experimental line intensity I^0 and the calculated line intensity I^*:

$$\Delta = \sum \ln^2 \left(\frac{I_i^*}{I_i^0} \right), \quad (18)$$

where i=1,2,$\cdots$ is the serial number of the line. The specific method of adjusting each parameter has been described in our previous work [41]. Due to space limitations, it will not be repeated here.

Table 3 shows the results of calibration-free quantitative analysis. The result of traditional CF was selected as the

Table 3 The quantitative analysis results of traditional CF and TICF under non-gated condition.

Element	Sample	Reference value (wt%)	CF		TICF	
			Measurement value (wt%)	Relative error (%)	Measurement value (wt%)	Relative error (%)
Al	1#	3.9	3.64	–6.46	3.85	–1.31
	2#	4.67	4.29	–7.83	4.51	–3.50
	3#	5.38	4.99	–6.98	5.29	–1.62
	4#	6.48	6.2	–4.12	6.63	2.25
	5#	6.78	6.43	–4.95	6.87	1.35
	Average	/	/	**6.07**	/	**2.01**
V	1#	5.65	6.54	18.17	5.65	0
	2#	5.01	5.4	10.09	4.95	–1.14
	3#	3.41	4.29	28.64	3.63	6.38
	4#	4.46	5.49	25.73	4.46	0
	5#	3.85	4.86	29.09	4.02	4.34
	Average	/	/	**22.34**	/	**1.92**

baseline for comparison, where the non-gated spectra was directly used to build traditional CF model. It can be seen that the newly proposed method TICF can significantly improve the measurement accuracy. Since the line intensity of Fe, Si and C were undetectable and their concentrations were relatively low, the prediction of these elements was neglected. In the future, more samples and more different types of samples can be tested to verify the applicability of the TICF method. For a set of different samples with similar matrix, only one preliminary time-resolved experiment is necessary to get the evolution trend of plasma parameters.

5 Conclusion

A time-integration calibration-free (TICF) method that can be used under non-gated conditions is proposed for laser-induced breakdown spectroscopy (LIBS). In order to eliminate the effects of temporal inhomogeneity of plasma, the parameters of the plasma are considered as functions of time but spatially homogeneous. The spectrum under non-gated conditions is regarded as the integration of the plasma emission along time. The line intensity at each moment of the plasma is calculated according to the profile of plasma evolution, and the self-absorption correction is performed separately for the line intensity at each moment. The application of TICF on titanium alloys shows that the elemental concentration measurement accuracy was significantly improved compared with traditional calibration-free method. The proposed TICF method considers the temporal inhomogeneity of plasma parameters, which extends the applicability of calibration-free for LIBS with non-gated detectors. Spatial inhomogeneity effects should be considered in the future to improve the performance further.

Acknowledgements The authors are grateful for the financial supports from National Natural Science Foundation of China (No. 51906124), Shanxi Province Science and Technology Department (No. 20201101013), Guoneng Bengbu Power Generation Co., Ltd. (20212000001), and Scientific Research Program for Young Talents of China National Nuclear Corporation (2020).

References

1. D. F. Andrade, E. R. Pereira-Filho, and D. Amarasiriwardena, Current trends in laser-induced breakdown spectroscopy: A tutorial review, *Appl. Spectrosc. Rev.* 56(2), 98 (2021)
2. Z. Wang, M. S. Afgan, W. Gu, Y. Song, Y. Wang, Z. Hou, W. Song, and Z. Li, Recent advances in laser-induced breakdown spectroscopy quantification: From fundamental understanding to data processing, *Trends Analyt. Chem.* 143, 116385 (2021)
3. L. B. Guo, D. Zhang, L. X. Sun, S. C. Yao, L. Zhang, Z. Wang, Q. Q. Wang, H. B. Ding, Y. Lu, Z. Y. Hou, and Z. Wang, Development in the application of laser-induced breakdown spectroscopy in recent years: A review, *Front. Phys.* 16(2), 22500 (2021)
4. Z. Wang, T. B. Yuan, Z. Y. Hou, W. D. Zhou, J. D. Lu, H. B. Ding, and X. Y. Zeng, Laser-induced breakdown spectroscopy in China, *Front. Phys.* 9(4), 419 (2014)
5. J. Li, M. Xu, Q. Ma, N. Zhao, X. Li, Q. Zhang, L. Guo, and Y. Lu, Sensitive determination of silicon contents in low-alloy steels using micro laser-induced breakdown spectroscopy assisted with laser-induced fluorescence, *Talanta* 194, 697 (2019)
6. S. Sheta, M. S. Afgan, Z. Hou, S. Yao, L. Zhang, Z. Li, and Z. Wang, Coal analysis by laser-induced breakdown spectroscopy: A tutorial review, *J. Anal. At. Spectrom.* 34(6), 1047 (2019)
7. S. Ma, Y. Tang, S. Zhang, Y. Ma, Z. Sheng, Z. Wang, L. Guo, J. Yao, and Y. Lu, Chlorine and sulfur determination in water using indirect laser-induced breakdown spectroscopy, *Talanta* 214, 120849 (2020)
8. Q. Li, W. Zhang, Z. Tang, K. Liu, C. Zhu, R. Zhou, K. Liu, and X. Li, Determination of fluorine content in rocks using laser-induced breakdown spectroscopy assisted with radical synthesis, *Talanta* 234, 122712 (2021)
9. R. Yuan, Y. Tang, Z. Zhu, Z. Hao, J. Li, H. Yu, Y. Yu, L. Guo, X. Zeng, and Y. Lu, Accuracy improvement of quantitative analysis for major elements in laser-induced breakdown spectroscopy using single-sample calibration, *Anal. Chim. Acta* 1064, 11 (2019)
10. Z. Hou, Z. Wang, L. Li, X. Yu, T. Li, H. Yao, G. Yan, Q. Ye, Z. Liu, and H. Zheng, Fast measurement of coking properties of coal using laser induced breakdown spectroscopy, *Spectrochim. Acta B At. Spectrosc.* 191, 106406 (2022)
11. S. Pagnotta, M. Lezzerini, B. Campanella, S. Legnaioli, F. Poggialini, and V. Palleschi, A new approach to non-linear multivariate calibration in laser-induced breakdown spectroscopy analysis of silicate rocks, *Spectrochim. Acta B At. Spectrosc.* 166, 105804 (2020)
12. W. Song, Z. Hou, W. Gu, H. Wang, J. Cui, Z. Zhou, G. Yan, Q. Ye, Z. Li, and Z. Wang, Industrial at-line analysis of coal properties using laser-induced breakdown spectroscopy combined with machine learning, *Fuel* 306, 121667 (2021)
13. V. C. Costa, M. L. de Mello, D. V. Babos, J. P. Castro, and E. R. Pereira-Filho, Calibration strategies for determination of Pb content in recycled polypropylene from car batteries using laser-induced breakdown spectroscopy (LIBS), *Microchem. J.* 159, 105558 (2020)
14. W. Gu, Z. Hou, W. Song, L. Li, X. Yu, J. Liu, Y. Song, M. S. Afgan, Z. Li, Z. Liu, and Z. Wang, Compensation for the variation of total number density to improve signal repeatability for laser-induced breakdown spectroscopy, *Anal. Chim. Acta* 1205, 339752 (2022)
15. J. J. Hou, L. Zhang, W. B. Yin, S. C. Yao, Y. Zhao, W. G. Ma, L. Dong, L. T. Xiao, and S. T. Jia, Development and performance evaluation of self-absorption-free laser-induced breakdown spectroscopy for directly capturing optically thin spectral line and realizing accurate chemical composition measurements, *Opt. Express* 25(19), 23024

(2017)
16. J. Dong, L. Liang, J. Wei, H. Tang, T. Zhang, X. Yang, K. Wang, and H. Li, A method for improving the accuracy of calibration-free laser-induced breakdown spectroscopy (CF-LIBS) using determined plasma temperature by genetic algorithm (GA), *J. Anal. At. Spectrom.* 30(6), 1336 (2015)
17. A. Ciucci, M. Corsi, V. Palleschi, S. Rastelli, A. Salvetti, and E. Tognoni, New procedure for quantitative elemental analysis by laser-induced plasma spectroscopy, *Appl. Spctroscopy* 53, 960 (1999)
18. S. Zhang, Z. Hu, Z. Zhao, F. Chen, Y. Tang, Z. Sheng, D. Zhang, Z. Zhang, H. Jin, H. Pu, and L. Guo, Quantitative analysis of mineral elements in hair and nails using calibration-free laser-induced breakdown spectroscopy, *Optik (Stuttg.)* 242, 167067 (2021)
19. E. Tognoni, G. Cristoforetti, S. Legnaioli, and V. Palleschi, Calibration-free laser-induced breakdown spectroscopy: State of the art, *Spectrochim. Acta B At. Spectrosc.* 65(1), 1 (2010)
20. A. Taleb, V. Motto-Ros, M. J. Carru, E. Axente, V. Craciun, F. Pelascini, and J. Hermann, Measurement error due to self-absorption in calibration-free laser-induced breakdown spectroscopy, *Anal. Chim. Acta* 1185, 339070 (2021)
21. E. Tognoni, G. Cristoforetti, S. Legnaioli, V. Palleschi, A. Salvetti, M. Mueller, U. Panne, and I. Gornushkin, A numerical study of expected accuracy and precision in calibration-free laser-induced breakdown spectroscopy in the assumption of ideal analytical plasma, *Spectrochim. Acta B At. Spectrosc.* 62(12), 1287 (2007)
22. L. Sun and H. Yu, Correction of self-absorption effect in calibration-free laser-induced breakdown spectroscopy by an internal reference method, *Talanta* 79(2), 388 (2009)
23. M. Qasim, M. Anwar-ul-Haq, A. Shah, M. Sher Afgan, S. U. Haq, R. Abbas Khan, and M. Aslam Baig, Self-absorption effect in calibration-free laser-induced breakdown spectroscopy: Analysis of mineral profile in Maerua oblongifolia plant, *Microchem. J.* 175, 107106 (2022)
24. D. M. Díaz Pace, R. E. Miguel, H. O. Di Rocco, F. Anabitarte García, L. Pardini, S. Legnaioli, G. Lorenzetti, and V. Palleschi, Quantitative analysis of metals in waste foundry sands by calibration free-laser induced breakdown spectroscopy, *Spectrochim. Acta B At. Spectrosc.* 131, 58 (2017)
25. A. Jabbar, Z. Hou, J. Liu, R. Ahmed, S. Mahmood, and Z. Wang, Calibration-free analysis of immersed metal alloys using long-pulse-duration laser-induced breakdown spectroscopy, *Spectrochim. Acta B At. Spectrosc.* 157, 84 (2019)
26. H. Shakeel, S. U. Haq, Q. Abbas, A. Nadeem, and V. Palleschi, Quantitative analysis of Ge/Si alloys using double-pulse calibration-free laser-induced breakdown spectroscopy, *Spectrochim. Acta B At. Spectrosc.* 146, 101 (2018)
27. E. Grifoni, S. Legnaioli, M. Lezzerini, G. Lorenzetti, S. Pagnotta, and V. Palleschi, Extracting time-resolved information from time-integrated laser-induced breakdown spectra, *J. Spectrosc.* 2014, 1 (2014)
28. Z. Hu, F. Chen, D. Zhang, Y. Chu, W. Wang, Y. Tang, and L. Guo, A method for improving the accuracy of calibration-free laser-induced breakdown spectroscopy by exploiting self-absorption, *Anal. Chim. Acta* 1183, 339008 (2021)
29. C. Aragón and J. A. Aguilera, Quantitative analysis by laser-induced breakdown spectroscopy based on generalized curves of growth, *Spectrochim. Acta B At. Spectrosc.* 110, 124 (2015)
30. I. B. Gornushkin, J. M. Anzano, L. A. King, B. W. Smith, N. Omenetto, and J. D. Winefordner, Curve of growth methodology applied to laser-induced plasma emission spectroscopy, *Spectrochim. Acta B At. Spectrosc.* 54(3–4), 491 (1999)
31. Y. Zhang, Y. Lu, Y. Tian, Y. Li, W. Ye, J. Guo, and R. Zheng, Quantitation improvement of underwater laser induced breakdown spectroscopy by using self-absorption correction based on plasma images, *Anal. Chim. Acta* 1195, 339423 (2022)
32. F. O. Bredice, H. O. D. Rocco, H. M. Sobral, M. Villagrán-Muniz, and V. Palleschi, A new method for determination of self-absorption coefficients of emission lines in laser-induced breakdown spectroscopy experiments, *Appl. Spectrosc.* 64(3), 320 (2010)
33. J. J. Hou, L. Zhang, Y. Zhao, Z. Wang, Y. Zhang, W. G. Ma, L. Dong, W. B. Yin, L. T. Xiao, and S. T. Jia, Mechanisms and efficient elimination approaches of self-absorption in LIBS, *Plasma Sci. Technol.* 21(3), 034016 (2019)
34. F. Rezaei, G. Cristoforetti, E. Tognoni, S. Legnaioli, V. Palleschi, and A. Safi, A review of the current analytical approaches for evaluating, compensating and exploiting self-absorption in laser induced breakdown spectroscopy, *Spectrochim. Acta B At. Spectrosc.* 169, 105878 (2020)
35. D. Bulajic, M. Corsi, G. Cristoforetti, S. Legnaioli, V. Palleschi, A. Salvetti, and E. Tognoni, A procedure for correcting self-absorption in calibration free-laser induced breakdown spectroscopy, *Spectrochim. Acta B At. Spectrosc.* 57(2), 339 (2002)
36. A. M. El Sherbini, T. M. El Sherbini, H. Hegazy, G. Cristoforetti, S. Legnaioli, V. Palleschi, L. Pardini, A. Salvetti, and E. Tognoni, Evaluation of self-absorption coefficients of aluminum emission lines in laser-induced breakdown spectroscopy measurements, *Spectrochim. Acta B At. Spectrosc.* 60(12), 1573 (2005)
37. C. Aragón and J. A. Aguilera, Direct analysis of aluminum alloys by CSigma laser-induced breakdown spectroscopy, *Anal. Chim. Acta* 1009, 12 (2018)
38. H. Y. Moon, K. K. Herrera, N. Omenetto, B. W. Smith, and J. D. Winefordner, On the usefulness of a duplicating mirror to evaluate self-absorption effects in laser induced breakdown spectroscopy, *Spectrochim. Acta B At. Spectrosc.* 64(7), 702 (2009)
39. A. Demidov, S. Eschlböck-Fuchs, A. Y. Kazakov, I. B. Gornushkin, P. J. Kolmhofer, J. D. Pedarnig, N. Huber, J. Heitz, T. Schmid, R. Rössler, and U. Panne, Monte Carlo standardless approach for laser induced breakdown spectroscopy based on massive parallel graphic processing unit computing, *Spectrochim. Acta B At. Spectrosc.* 125, 97 (2016)
40. Z. Zhu, J. Li, Y. Guo, X. Cheng, Y. Tang, L. Guo, X.

Li, Y. Lu, and X. Zeng, Accuracy improvement of boron by molecular emission with a genetic algorithm and partial least squares regression model in laser-induced breakdown spectroscopy, *J. Anal. At. Spectrom.* 33(2), 205 (2018)

41. T. Li, Z. Hou, Y. Fu, J. Yu, W. Gu, and Z. Wang, Correction of self-absorption effect in calibration-free laser-induced breakdown spectroscopy (CF-LIBS) with blackbody radiation reference, *Anal. Chim. Acta* 1058, 39 (2019)
42. H. Sobral, G. Quintana-Silva, and A. Robledo-Martinez, Time-resolved optical characterization of the interaction between a laser produced plasma and a spark discharge, *Spectrochim. Acta B At. Spectrosc.* 167, 105844 (2020)
43. M. Dong, X. Mao, J. J. Gonzalez, J. Lu, and R. E. Russo, Time-resolved LIBS of atomic and molecular carbon from coal in air, argon and helium, *J. Anal. At. Spectrom.* 27(12), 2066 (2012)
44. Y. T. Fu, W. L. Gu, Z. Y. Hou, S. A. Muhammed, T. Q. Li, Y. Wang, and Z. Wang, Mechanism of signal uncertainty generation for laser-induced breakdown spectroscopy, *Front. Phys.* 16(2), 22502 (2021)
45. G. C. He, X. L. Zhu, L. N. Shi, S. J. Zhao, and Y. L. Hua, The self-absorption temporal evolution of spectral lines emitted from laser-induced plasmas, *Opt. Laser Technol.* 143, 107324 (2021)
46. N. Konjević, Plasma broadening and shifting of non-hydrogenic spectral lines: Present status and applications, *Phys. Rep.* 316(6), 339 (1999)
47. T. Q. Li, S. Sheta, Z. Y. Hou, J. Dong, and Z. Wang, Impacts of a collection system on laser-induced breakdown spectroscopy signal detection, *Appl. Opt.* 57(21), 6120 (2018)
48. Y. Yang, X. Hao, and L. Ren, Correction of self-absorption effect in calibration-free laser-induced breakdown spectroscopy(CF-LIBS) by considering plasma temperature and electron density, *Optik (Stuttg.)* 208, 163702 (2020)
49. I. B. Gornushkin, T. Völker, and A. Y. Kazakov, Extension and investigation by numerical simulations of algorithm for calibration-free laser induced breakdown spectroscopy, *Spectrochim. Acta B At. Spectrosc.* 147, 149 (2018)
50. G. Cristoforetti, A. De Giacomo, M. Dell'Aglio, S. Legnaioli, E. Tognoni, V. Palleschi, and N. Omenetto, Local thermodynamic equilibrium in laser-induced breakdown spectroscopy: Beyond the McWhirter criterion, *Spectrochim. Acta B At. Spectrosc.* 65(1), 86 (2010)
51. L. C. L. Borduchi, D. M. B. P. Milori, and P. R. Villas-Boas, Study of the effects of detection times in laser-induced breakdown spectroscopy and missed variation of plasma parameters with gate width, *Spectrochim. Acta B At. Spectrosc.* 191, 106409 (2022)